Screening and design of inhibitor scaffolds for the antibiotic resistance oxacillinase-48 (OXA-48) through surface plasmon resonance screening

Bjarte Aarmo Lund[1], Tony Christopeit[1], Yngve Guttormsen[2], Annette Bayer[2] and Hanna-Kirsti S. Leiros[1]*

[1]The Norwegian Structural Biology Centre (NorStruct), Department of Chemistry, UiT The Arctic University of Norway, Tromsø, Norway

[2]Department of Chemistry, UiT The Arctic University of Norway, Tromsø, Norway

ABSTRACT: The spread of antibiotic resistant bacteria is a global threat that shakes the foundations of modern healthcare. β-Lactamases are enzymes that confer resistance to β-lactam antibiotics in bacteria and there is a critical need for new inhibitors of these enzymes for combination therapy together with an antibiotic. With this in mind, we have screened a library of 490 fragments to identify starting points for the development of new inhibitors of the class D β-lactamase oxacillinase-48 (OXA-48), through Surface Plasmon Resonance (SPR), dose-rate inhibition assays and X-ray crystallography. Furthermore, we have uncovered structure-activity relationships and used alternate conformations from a crystallographic structure to grow a fragment into a more potent compound with a K_D of 50 μM and an IC_{50} of 18 μM.

Introduction

Each year infections with antibiotic resistant bacteria cause an estimated 25 000 deaths in Europe.[1] Thus there is a pressing need for new strategies to treat such infections. Today, the most commonly used antibiotics are β-lactam antibiotics such as penicillins, cephalosporins and carbapenems. However, there have not been any major developments since the introduction of carbapenems in 1976,[2] and many bacteria have become resistant to virtually all β-lactam antibiotics. A major resistance mechanism to β-lactam antibiotics is the expression of β-lactamases, enzymes able to hydrolyze the β-lactam ring, which renders the drug inactive.

A prevalent β-lactamase which has caused outbreaks of antibiotic resistant bacteria all over the world is OXA-48, an oxacillinase belonging to the Ambler class D of β-lactamases.[3,4] β-Lactamases belonging to this group have a serine in the active site similarly to the class A and C β-lactamases,[5] but show distinct properties such as dimerization[6] and a carboxylated lysine in the active site.[7] The carboxylated lysine is believed to play an important role in the β-lactam hydrolyze by acting as the general base responsible for activating the nucleophilic hydroxyl-group of the catalytic serine as well as activating the water responsible for deacetylating the complex.[8] The hydrophobic environment in the interior of the protein stabilizes the carboxylated lysine, but the pH has to be close to neutral or higher for the lysine to be non-protonated and amenable to carboxylation.[7] Without the carboxylation of the lysine there is a significant decrease in activity, and the decarboxylated enzyme appears to be inhibited by chloride ions.[7] OXA-48 is able to hydrolyze a wide range of antibiotics like penicillins and carbapenems, but is less efficient against expanded-spectrum cephalosporins.[3]

The co-administration of β-lactamase inhibitors together with β-lactam antibiotics has been a successful strategy to overcome resistance caused by class A and C β-lactamases.[9] The recent

approval of avibactam, a non β-lactam β-lactamase inhibitor binding covalently to the active site serine, showed that this strategy is also successful for class D β-lactamases. [10–13] However, reports of avibactam-resistance for class A and C β-lactamases have been published[14–16] and even though no avibactam-resistance for OXA-48 has been reported yet, there is a clear need for novel β-lactamase inhibitors as additional treatment method when resistance arises.

Fragment based drug discovery (FBDD) has been a successful approach in generating drug leads for several now marketed drugs.[17] In FBDD, a set of so-called fragments, small molecules with favorable physicochemical properties and a molecular weight below 300 Da, is screened. Generally, the affinity of fragment hits is low compared to hits from traditional high-throughput screenings. Hence, fragment hits have to be further optimized into potent inhibitors by linking, evolving or growing.[18] An additional advantage of FBDD is that derivatives and analogous compounds are often commercially available, enabling rapid determination of structure-activity relationships.[19]

Surface plasmon resonance (SPR)-based biosensor assays allow direct measurements of protein-ligand interactions. Furthermore, they are a useful tool to characterize such interactions by determining the kinetic parameters and the affinity.[19] SPR-based methods are also easily automated and the consumption of both protein and ligand is low.[20] Hence, SPR based assay are widely used in drug discovery to screen fragment libraries. A common challenge in FBDD are Pan-Assay Interference compounds (PAINS) that causes interference across different targets while being unlikely to progress into a potent and selective compound.[21] SPR-based assays are suitable to identify promiscuous binders and hence can avoid problems caused by PAINS. By using an orthogonal screening strategy, such as combining a biochemical assay together with an SPR assay, it is possible to identify likely PAINS.[20,22,23]

In this study, we report the results of screening a library of 490 fragments using SPR as the primary assay. Fragment hits from this primary screen were confirmed in a secondary biochemical enzymatic assay using the substrate nitrocefin. Furthermore, for several of the identified fragments, the crystal structure in complex with OXA-48 was determined. One of the fragments was further optimized into an inhibitor with increased potency.

Results and discussion

Cloning, protein expression and purification of His-TEV OXA-48

Two different OXA-48 gene constructs were used throughout this study. The first construct, referred to as nOXA-48, was expressed with the native signal sequence and purified from the periplasm as previously described.[24]

In order to increase the yield of OXA-48, a second gene construct was designed and expressed, and is henceforth referred to as tOXA-48. In this construct, the signal peptide (residues 1-22) as predicted by SignalP[25] was removed and a His-tag and a Tobacco Etch Virus (TEV) cleavage site were added. The tOXA48 construct was cloned and expressed in *Escherichia coli*. The protein was purified using the His-tag. The incorporation of a TEV cleavage site allowed for removal of the His-tag by TEV protease, leaving only one additional alanine at the N-terminus of tOXA-48. A second purification step separated cleaved protein from the uncleaved protein, followed by polishing by cation exchange chromatography. As judged by SDS PAGE analysis the protein was purified to homogeneity. Expression of tOXA-48 yielded approximately 10 mg of protein per liter of culture. Furthermore, the use of autoinduction-media reduced the hands-on time during expression since there was no need to monitor the optical density prior to induction.

Enzyme characterization and DMSO tolerance of nOXA-48

Analysis of the kinetic parameters of nOXA-48 with five β-lactam substrates and two reporter substrates (Table 1) show that nOXA-48 is able to hydrolyze carbapenems and penicillins. There has been several reports with steady-state kinetics for OXA-48,[26,27] and our results mirror the overall trends. The penicillins are quickly hydrolyzed, while the cephalosporins cefepime and CENTA are poorly hydrolyzed. nOXA-48 is less active against the carbapenems than against the penicillins. An exception is that nOXA-48 is very active against the cephalosporin substrate nitrocefin. However, nitrocefin is known to be easily hydrolysable due to its conjugated ringsystems.[28] For nOXA-48, the kinetic parameters were determined for the hydrolyzation of nitrocefin. The determined k_{cat} and K_m were similar to the values determined for tOXA-48, indicating that there were no significant differences in enzyme activity for the two different gene constructs nOXA-48 and tOXA-48.

Nitrocefin and CENTA are common reporter substrates to monitor the activity of β-lactamases. As nitrocefin is expensive and not stable in aqueous solutions, CENTA has been recommended for its favorable chemical properties and lower price.[29] However, our comparison (Table 1) shows that nOXA-48 is most efficient against nitrocefin, and that higher concentration of the CENTA substrate were necessary for detection, limiting the sensitivity of the assay. Hence, it was decided to use inhibition assay based on nitrocefin for the following fragment screening.

Since all fragments were solved in DMSO, it was necessary to investigate the influence of DMSO on the activity of nOXA-48. In our hands, nOXA-48 was tolerated up to 2.5% DMSO without significant loss in activity towards the hydrolysis of nitrocefin (data not shown).

Dilution-series for the β-lactamase inhibitor avibactam showed 50% inhibition at 1.5 μM after 5 minutes of incubation. Avibactam is known to bind covalently,[10] and covalent

inhibitors are time-dependent in their dose-response, however the results do validate that the assay is sensitive to inhibitor measurements and can be used for the fragment screening.

Establishing SPR assay and the influence of bicarbonate

To our knowledge, we present the first SPR-experiments for OXA-48. Since SPR allows for both measurements of affinity and determination of kinetic parameters, it is a very useful technique for drug design. The tOXA-48 protein was immobilized to the senor surface by amine coupling resulting in a stable surface. Although immobilization levels up to 10000 RU could be reached, only approximately 5000 RU were immobilized to reduce bulk effects and avoid mass transport limitations.[30]

To verify the enzyme integrity on the chip, the interaction with the substrate meropenem was investigated (Figure 1). Meropenem clearly bound to the enzyme showing that the enzyme retains activity after immobilization. However, the substrate release was very slow. Based on the report of oxacillinases dependence on bicarbonate[7] we hypothesized that the absence of bicarbonate in the running buffer leads to a decarboxylation of Lys73 causing the slow dissociation of the substrate. By including 50 mM bicarbonate ($NaHCO_3$) in the running buffer the rate of disassociation increased dramatically as shown in Figure 1. This indicates that adding bicarbonate to the buffer is essential to maintain the enzyme active through a carboxylated Lys73.

With bicarbonate included in the running buffer, we were able to determine the affinity and kinetic parameters for meropenem using a 1:1 binding model Figure 1 yielding a k_a of 4 × 10^4 $M^{-1}s^{-1}$, a k_d of 0.3463 s^{-1} and K_D of 0.85 µM. This K_D value compares well with the K_m of 1.0 µM for meropenem found in the characterization of nOXA-48 (Table 1). Thus, the similar K_D and K_m determined by the two different methods supporting that the protein coupled to the CM5 SPR chip in the SPR experiment is active.

Orthogonal fragment screening with a primary biophysical screening and a secondary biochemical screening

The screening strategy was designed to minimize the risk of false positives by using two orthogonal assays. An SPR based assay was used as primary screen to identify binders from our 490 compound subset from the Maybridge Ro3 collection and the secondary screen measured the inhibition potency against the substrate nitrocefin. All the fragments adhere to the "rule of three".[31]

The primary screening at a single concentration (300 µM) identified 84 fragments, with binding to the protein. These 84 fragments were analyzed in a dilution-series (118 – 900 µM). Among these, 77 compounds showed concentration-dependent and reversible binding to the tOXA-48 surface. The other fragments exhibited very slow disassociation, no clear concentration dependency or superstoichometric binding which are common signs of unspecific binding[19,22] and were therefore rejected.

The SPR based assay only identifies binders and in order to determine whether the binders were inhibitors, we performed a secondary screening for all the 77 binders using a biochemical inhibition assay against nitrocefin using nOXA-48. We were able to determine IC_{50} values (Figure 3) for 10 of the fragments. The remaining compounds did not have the inhibitory potency necessary to give reliable IC_{50}-values in our assay, and were not considered good starting points for further inhibitor optimization.

The K_D values were calculated based on the SPR results for 8 of the fragments with highest potency (Figure 2). For compound **4** and **5**, the steady state values showed a linear concentration dependency and hence, it was not possible to determine the K_D. The linear concentration dependency is most likely caused by a combination of specific and non-specifc interaction with the protein. However, the signal intensities were in the range expected for a

1:1 interaction based on Equation 1 and therefore the compounds were not rejected. Some

fragments may also bind to other sites on the enzyme without influencing the activity, which

could explain the higher number of compounds binding in the SPR experiments without the

corresponding inhibition effect in the competitive nitrocefin experiment.

$$R_{max} = \frac{fragment\ MW}{enzyme\ MW} \times immobilization\ level$$
$\qquad\qquad$ Equation 1

Overall there is a good agreement between the affinities (K_D) measured by SPR and the IC_{50}

values determined from the biochemical assay (Table 2), except for compounds **8** and **9**

which had higher IC_{50} values than expected from the K_D values. There were differences in the

buffers that may explain the differences. We kept the buffer for the biochemical assay

identical to the kinetics buffer, except for the addition of 2.5% DMSO. Whereas for the SPR

assay, we prioritized having the conditions similar to the crystallization conditions to

increase the probability of obtaining X-ray crystallographic complex-structures of hits.

Ligand efficiency (LE) is a simple parameter for hit assessment, which scales the affinity

with the number of non-hydrogen atoms to overcome the bias towards ligands of high

molecular weight.[32] Overall, the identified hits had good affinities (Table 2), and the

calculated LE-values are within the range of what is expected of fragment-hits.[33]

In summary, the ten fragments are all interesting starting points for further inhibitor

development after the screening.

X-ray structures of tOXA-48 with compound 1, 2 and 3 and structure activity relationships

Atomic resolution details from the inhibition mode of tOXA-48 were found by soaking apo

tOXA-48 crystals with the 10 fragment hits. By this procedure, we obtained crystal structures

of tOXA-48 in complex with 3 of the fragments. All structures have four molecules in the asymmetric unit, but crystalized in two different space groups ($P2_12_12_1$ and $P2_1$). For the new tOXA-48 structures the RMSD was below 0.4 Å compared to the published apo structure of nOXA-48 (PDB ID: 3HBR) as calculated by the protein structure comparison service PDBeFold at EBI (http://www.ebi.ac.uk/msd-srv/ssm).[34] The low RMSD between our tOXA-48 and the apo nOXA-48[27] indicate very similar structures, and that our structures equally well describe the OXA-48 drug target. Refinement statistics are summarized in Table 4. Our new tOXA-48 structures all have carboxylated Lys73 residues (Kcx73) similar to e.g. nOXA-48 (PDB ID: 3HBR) as one would expect with the neutral pH.[27]

All the compounds are anchored near the active site Ser70, which explains the competitive inhibition mode of these fragments.

From the crystal structure complexes of tOXA-48 and compounds **1**, **2** and **3**, it is clear that the carboxylate groups have ionic interactions with the sidechain of Arg250 and a charge induced hydrogen bond to sidechain oxygen of Thr209. This is consistent with the role Arg250 has in substrate binding,[35,36] and similar to the interaction between the negatively charged sulfate group of avibactam to Arg250 in nOXA-48 (PDB ID: 4WMC) and the equivalent Arg261 in OXA-24 (PDB ID:4WM9).[12,37] All the ten hits (compounds **1-10**) are carboxylates, and since the SPR and IC_{50} experiments are performed at pH 7.0, the compounds are all likely to be negatively charged. The removal of the carboxylate group abolished binding, as seen for compound **11**, which had no activity. Compound **14**, which has a ketone functionality instead of the carboxylate group, also showed weak inhibition (Table 3). This shows that the carboxyl group forms interactions crucial for the fragment binding.

Compound **1**, **2** and **3** had the highest affinity. These fragments are structurally related to each other with 3-substituted benzoic acids as a common feature. Compounds **4** and **10**

resemble compounds **1-3**, but contain an additional linker, which appears to be detrimental to the inhibition.

Compound **1** bound to tOXA-48 (tOXA-48:**1**; Figure 4A) was observed in multiple conformations. The conformation shown in Figure 4B is facing out of the active-site and has hydrophobic interactions with Trp105, Thr209, Gly210, Tyr211 and Leu247. The carboxylate-group makes ionic bonds to Arg250 ($d(O_{ligand}...N_{R250})$ = 2.5-3.1Å). The pyridine-nitrogen also makes a hydrogen-bond to a water-molecule ($d(O_{ligand}...O_{water})$ = 2.5 Å). The conformation shown in Figure 4C is more buried, and has hydrophobic interactions with Val120, Leu158 and Tyr211. The carboxylate group in this conformation makes only a single ionic bond with Arg250 ($d(O_{ligand}...N_{R250})$ = 3.4Å), but also makes a water-mediated hydrogen-bond to Thr209.

However, compound **2** (tOXA-48:**2**; Figure 4D)**,** which only differs in the position of the N atom of the pyridine ring, crystallized in a single conformation in the 4 protein monomers in the asymmetric unit corresponding to the conformation in Figure 4B. The compound makes several hydrophobic interactions with Ser70, Ile102, Ser118, Gly210 and Tyr211. The carboxylate group forms ionic bonds with Arg250 ($d(O_{ligand}...N_{R250})$ = 3.1-3.2Å), and a hydrogen-bonds with Thr209 ($d(O_{ligand}...O_{T209})$ = 3.1Å), as well as water-mediated hydrogen-bonds with both Arg250 and Thr209.

Compound **3** (tOXA-48:**3**; Figure 4F**)** also shares the same overall conformation and has Π-Π interactions with Tyr211 (5.3 Å) and hydrophobic interactions with Ser70, Ile102, Trp105, Ser118, Thr209, Gly210 and Leu247. The carboxylate forms ionic bonds with Arg250 (($d(O_{ligand}...N_{R250})$ = 2.5-3.0 Å).

There is no significant difference in activity between compound **1**, **2** and **3** (Table 2). Furthermore, compound **12** (Table 3) also shows that the nitrogen on the pyridine-ring is not

critical for activity; while the nitrogen is useful to maintain solubility. This gives an indication that the pyridine/thiazole ring may be modified.

To investigate if the pyridine/thiazole ring was necessary for binding, as it was not clear which interactions the second ring made, compound **15** and **16** were both tested and gave very weak inhibition (Table 3). This shows that while we could modify the pyridine/thiazole ring without losing activity, it is not beneficial to remove them. However, the addition of an amine group in compound **13** did not significantly alter the activity, which shows that the second ring may have good exit vectors.

Compounds **5-9** contain indol- or quinoline moieties as a common feature. Among these, compound **5** and **6** have the highest potency, but the LE is higher for compounds **7**, **8** and **9**. Unfortunately, no clear density could be observed for these compounds in soaking-experiments, indicating that the binding mode is too flexible to be observed by X-ray crystallography.

Hit-optimization by organic synthesis

In the crystal structure of compound **1** bound to tOXA-48 we found two different fragment conformations as illustrated in Figure 4A and Figure 4B. By structurally merging the two different conformations of the pyridine ring, compound **17** was designed. Docking using GLIDE indicated that compound was able to bind to the enzyme with higher affinity as compared to compound **1**, and decided to pursue the synthesis of compound **17** based on these results. A Suzuki coupling of 3,5-dibromobenzoic acid with 4-pyridylboronic acid provided compound **17** (Scheme 1) in excellent yield (96%) and good purity (>99%) as determined by HPLC analysis.

The SPR based assay was used to determine the K_D of 50 µM (Figure 5), with a LE of 0.29 kcal per mole per heavy atom, and the enzyme inhibition assay was used to determine the IC_{50} of 18 µM for compound **17**.

The crystal structure of compound **17** bound to tOXA-48 (tOXA-48:**17**; Figure 5D) shows that it overlaps with two of the conformations observed for compound **1**, which validated our approach of merging alternate conformations. Compound **17** forms hydrophobic interactions with Ser70, Ile102, Val120, Tyr211, Ser244 and Leu247, and there is an additional water-mediated (W3) hydrogen bond to Arg214. This water-network was not observed for the other compounds, but this could be due to the lower resolution of these structures. Compound **17** forms ionic bonds to Arg250 (($d(O_{ligand}...N_{R250}) = 2.8$-$2.9$ Å), and water-mediated hydrogen bonds to both Ser118 (W1) and Thr209 (W2) and with an intricate water-network revealed by the high resolution of this structure.

There is still a need to investigate the possible exit vectors of compound **17**, however compound **17** shows that for this class of compounds it is possible to optimize inhibitor propensity in terms of higher enzyme affinity and demonstrates that alternate conformations may be used as a tool in structure guided drug design.

Based on a sequence alignment of the class D β-lactamase family[38] it is reasonable to believe that compound **17** would have potential to inhibit the majority of the family. Ala69, Trp105, Val120, Leu158, Thr209 and Arg250 are all conserved (>80% of the family-members), and in many of the cases the amino acid substitutions might be compatible with the same interactions.

It is interesting to compare the results of this study with the inhibitor scaffolds identified for the Ambler class B metallo-β-lactamase VIM-2 [3,4] from similar experiments.[39] Several of the hits overlap and more than half of the hits identified are carboxylates. While there is no

significant sequence identity between the different classes of β-lactamases, both enzymes OXA-48 and VIM-2 are capable of hydrolyzing the same substrates, and could potentially be inhibited by the same compounds. Incidentally, compound **17** also shows some activity against VIM-2 (data not shown), opening the possibility of a pan β-lactamase inhibitor.

Conclusions

In this study, we have done a fragment screening for new inhibitor scaffolds of the class D β-lactamase OXA-48. From a total of 490 screened fragments, 10 compounds could be confirmed by two orthogonal screens, SPR and enzyme inhibition assay, to bind and inhibit OXA-48. Three X-ray crystallographic structures established the binding modes of these fragments. One compound was further optimized by merging two observed conformations in two different protein chains in the X-ray structure of fragment **1** (tOXA-48:**1**). This resulted in a more potent inhibitor with a K_D of 50 μM and IC_{50} value 18 μM compared to 280 μM (K_D) and 250 μM (IC_{50}) respectively for compound **1**, thus validating that our reported inhibitor scaffolds based on heterocycles with a single carboxylate group have potential for further development into more potent inhibitors for the antibiotic resistance enzyme OXA-48.

Experimental Section

General procedures: As long as not otherwise stated chemicals were purchased from Sigma-Aldrich, and used as received. Compound **13** were purchased from Fluorochem (UK) and compound **14** from Enamine (USA). All chemicals were of analytical quality. Residues are numbered according to the apo OXA-48 structure (PDB ID:3HBR).

Cloning, protein expression and purification of His-TEV OXA-48(tOXA-48)

Native full-length OXA-48 with the native leader sequence was expressed and purified from the periplasm as previously described,[24] and is referred to as nOXA-48.

In addition, a new His-TEV OXA-48 gene construct was cloned by introducing a hexa-histidine tag together with a TEV protease cleavage site while removing the predicted native leader sequence (residues 1-22) from SignalP.[25] This construct is henceforth called tOXA-48. The cloning was done similarly to the native full-length OXA-48 using exponential megapriming PCR cloning,[24,40] however, the insertion of the TEV protease site required multi-component assembly.[41] All primers (Sigma-Aldrich, Table 5) were desalted and dissolved to 100 µM in nuclease-free water.

The new tOXA-48 construct was transformed into in house modified *E. coli* strain BL21 Star (DE3) pRARE and expressed in the autoinduction media ZYP-5052[42] with ampicillin (100 mg/L) and chloramphenicol (34 mg/L). 3-4 hours after inoculation at 37 °C, the temperature was reduced to 25 °C to allow low temperature induction overnight. Pelleted cells were frozen, later thawed and sonicated. The lysate was cleared by centrifugation (50 000×g, 4 °C, 30 min), then loaded on a 1 mL HisTrap FF crude column equilibrated with 25 mM HEPES pH 6.5 and 50 mM K_2SO_4. The tOXA-48 was eluted with a linear gradient over 30 column volumes to 500 mM imidazole, 25 mM HEPES pH 6.5 and 50 mM K_2SO_4. Fractions with tOXA-48 were cleaved overnight with 1:10 ratio of in-house produced His-tagged TEV protease to tOXA-48, during dialysis against 25 mM HEPES pH 6.5, 25 mM K_2SO_4, 1 mM EDTA and 2 mM 2-mercaptoethanol. The dialyzed sample was loaded on a second HisTrap column, and the flow-through examined for cleaved tOXA-48, with the His-tagged TEV-protease, uncleaved protein and contaminants bound to the column. A 5 mL cation exchange

(HiTrap SP HP) column was used for a final polishing step with a gradient from 25 mM HEPES pH 6.5 to 25 mM HEPES pH 8.5 with 150 mM K_2SO_4.

Fragment library

490 fragments were purchased from the Maybridge Ro3 collection. All compounds were dissolved in 100% DMSO to a concentration of 150 mM. These stock liquids and powders were kept at 4 °C, while aliquot samples were kept at -20 °C. All fragments in the library had a molecular weight between 80 and 300 Da, a cLogP $\leq$ 3, the number of H-bond acceptors and donors was $\leq$ 3 and the number of rotatable bonds was $\leq$ 3.

Biochemical studies: enzyme kinetics, DMSO tolerance and inhibition studies

All experiments were performed using a Spectramax M2e at 25 °C. Initial velocities were determined in the SoftMax Pro software (Molecular Devices). All experiments were done with a volume of 100 µL.

Michaelis-Menten kinetics were first established for the chromogenic β-lactam substrate nitrocefin in the kinetics buffer with 100 mM Na_2HPO_4/NaH_2PO_4 (pH 7.0), 50 mM $NaHCO_3$ and 0.2 mg/ml BSA as previously described.[26] Then additional substrates were examined: ampicillin ($\Delta\varepsilon_{235 \text{ nm}}$ = -820 M^{-1} cm^{-1}, 16-2000 µM, 1nM nOXA-48), benzylpenicillin ($\Delta\varepsilon_{235 \text{ nm}}$ = -775 M^{-1} cm^{-1}, Panpharma,176-3000 µM, 100pM nOXA-48), cefepime ($\Delta\varepsilon_{260 \text{ nm}}$ = -10000 M^{-1} cm^{-1}, 26-450 µM, 1nM nOXA-48), CENTA ($\Delta\varepsilon_{405 \text{ nm}}$ = 6400 M^{-1} cm^{-1}, Calbiochem, 2-300 µM, 20 nM nOXA-48), meropenem ($\Delta\varepsilon_{300 \text{ nm}}$ = -6500 M^{-1} cm^{-1}, 1-11 µM, 140 nM nOXA-48), nitrocefin ($\Delta\varepsilon_{482 \text{ nm}}$ 17400 M^{-1} cm^{-1}, Calbiochem, 10-300 µM, 1 nM nOXA-48 and tOXA-48) and imipenem ($\Delta\varepsilon_{300 \text{ nm}}$ = -9000 M^{-1} cm^{-1}, 1-100 µM, 1 nM nOXA-48). The reactions were started by the addition of enzyme. The linear phase of the reaction time course was used to determine the steady-state velocities. The observed rate constants (k_{obs} =

$v/[E]$) as a function of the substrate concentrations were used to determine k_{cat} and K_m with non-linear regression in GraphPad Prism 6 (GraphPad Software).

DMSO tolerance was established with dilution-series of DMSO concentrations from 0.15-10% using 25 µM nitrocefin as the reporter substrate.

Avibactam (AstraZeneca) in dilutions from 50 nM – 20 µM were tested in a competition experiment with 25 µM nitrocefin and 100 pM nOXA-48 to validate the sensitivity of the assay for inhibitors. Fragments identified in the primary screen by stronger signal than the reference surface, were tested at a single concentration of 750 µM with 25 µM nitrocefin and 100 pM nOXA-48. Duplicates were done, and for fragments with more than 10% deviation triplicates were run. Avibactam and the fragments were incubated with the enzyme for approximately 5 minutes before the experiments were started by the addition of nitrocefin. For the inhibition testing DMSO was included in the kinetics buffer to a final concentration of 2.5%.

Dose-response IC_{50} values were determined for fragments with $\geq$50% inhibition at 750 µM, with fragment-concentrations from 7.3 µM-1.9 mM in 9 dilutions in a competition experiment with 25 µM nitrocefin. The $\log_{10}$ of the inhibitor concentrations to the response with bottom and top constant based on controls were fitted non-linearly in GraphPad Prism 6 (GraphPad Software) to determine the IC_{50}-value. The Hill-constant was kept constant at 1.

Surface plasmon resonance (SPR) interaction studies: primary screening and K_D measurements

All SPR experiments were performed on a Biacore T200 at 25°C. The data were analyzed using Biacore T200 Evaluation Software 2.0 (GE Healthcare). The sensorgrams were double reference subtracted using a reference surface and blank injections.

tOXA-48 was diluted to 25 µg/mL in 10 mM MES pH 5.5. The enzyme was immobilized to a level of around 5000 RU on a CM5-chip using standard amine coupling.

For the interaction studies with Meropenem, the final running buffer included 25 mM HEPES pH 7.0, 50 mM K_2SO_4, 0.5% Tween-20, 50 mM $NaHCO_3$ and 2.5% DMSO. The K_D was calculated from the sensorgrams recorded with 62.5 nM-32 µM meropenem using the 1:1 binding kinetics model. The flow rate was 30 µL/min and with a contact time of 60 s and 240 s disassociation time.

In the primary screening, each fragment was tested twice in two independent experiments, with reverse sample order in the second run. The fragment concentration was 300 µM with 30 s contact time and 15 s disassociation time. The fragments were diluted with running buffer without DMSO to maintain a constant DMSO concentration of 2.5%. Flow rate was 30 µL/min and the flow system was washed with 50% DMSO between each sample.

Positive controls (meropenem) were tested every 12th cycle to ensure active enzyme together with blanks (running buffer), and solvent-correction with a DMSO-gradient (1.5-4%) was performed every 48th cycle. Seven startup cycles with running buffer were performed. No surface regeneration was done, and protein was immobilized to a new flow-channel when the ratio of the response to control surface was significantly lowered.

For testing fragments in concentration series, they were tested in a dilution-series with six concentrations from 118-900 µM. Seven startup cycles with buffer were performed. A positive control (meropenem) was used for every 30th cycle and a negative control with buffer was used for every 30th cycle. Solvent correction with varying DMSO concentration was performed every 45th cycle. Affinities were calculated from the steady-state affinity model with a constant R_{max} adjusted by the control and molecular weight of the fragment. The same protocol was used for the compounds **11-17**, with the exception that compound **17** had 10 dilutions with concentrations from 1.8-900 µM.

Crystallization, soaking and X-ray data collection

Crystals of tOXA-48 were obtained by vapor diffusion technique in a manual hanging drop setup. tOXA-48 at 8 mg/mL was mixed with reservoir solution containing 0.1 M HEPES pH 7.5, 10% PEG 8000 and 4-8% 1-butanol as previously published[12] with a drop-ratio of 1.5:2.5 µL for protein:reservoir.

Fragments were diluted to 3.75 mM in the cryo solution with 0.1 M HEPES pH 7.5, 10% PEG 8000, 5% 1-butanol and 25% ethanediol and crystals were soaked for two hours (OXA-48:**1**) or 16-18 hours (OXA-48:**2**, OXA-48:**3** OXA-48:**17**). Then the crystals were flash cooled in liquid nitrogen. In total 10 fragments were soaked (all from Table 2) but tOXA-48 complex structures were only obtained for compound **1, 2, 3** and later with compound **17**.

X-ray diffraction data were collected at the BL 14.1 and 14.2 beamlines at BESSY (Berlin, Germany). The data was integrated in XDS.[43] The datasets were scaled and merged in AIMLESS.[44]

Molecular replacement was performed with PHASER[45] with the nOXA-48 apo structure (PDB ID: 3HBR)[27] as search model to obtain initial phases.

Electron density could be seen for three fragments and compound **17** after initial refinement in PHENIX[46] when automatically added waters were removed from the active site and the difference Fourier electron density maps recalculated. Restraints for the fragments were prepared using the GRADE webserver,[47] the fragments were placed manually using COOT,[48] and the final refinements were done in PHENIX. Omit-maps were calculated using the phenix.polder-tool.[46,49] Figures were made using PyMOL[50] and LigPlot+[51].

Docking of compound 17

The structure of tOXA-48:**1** was used as a starting model. The protein preparation wizard in Maestro was used to add hydrogens, assign bond orders, delete waters and optimize the hydrogen bond network. A docking grid was prepared using the coordinates of compound **1** as the centroid. Compound **17** was prepared using the Ligprep tool to generate 3D coordinates, optimize geometries and assign ionization states. Compound **17** was docked using the induced fit protocol[52] in the Schrödinger suite 2013-1 with no constrains defined and with residues within 5 Å of the binding pose refined.

Organic synthesis of compound 17

Compound **17** was prepared in analogy to literature (Scheme 1).[53] 3,5-Dibromobenzoic acid (228 mg, 0.81 mmol, 1 equiv), 4-pyridylboronic acid (300 mg, 2.4 mmol, 3 equiv) and potassium phosphate (1.04 g, 4.9 mmol, 6 equiv) were dissolved in dioxane (6 mL) and water (6 mL). The solution was degassed by vacuum/Argon cycles (10 times) before addition of $PdCl_2(PPh_3)_2$ (57 mg, 81 μmol, 10 mol%) and further degassing (5 times). The resulting mixture was stirred at 95 °C under an Argon atmosphere for 16 hours, after which HRMS in negative mode showed only bi-coupled benzoic acid. The reaction mixture was filtered and diluted with water (30 mL) before washing with chloroform (3×30 mL). The aqueous phase was concentrated on a rotary evaporator and applied to a Biotage snaplet precolumn. On a

Biotage SP1 automated flash system, the compound was purified by a 60 g C18 Biotage SNAP column with a gradient of 0-100% acetonitrile in water to yield the compound **17** as a white solid (215 mg, 0.78 mmol, 96%). An aliquot of the solid was redissolved in ethyl acetate and QuadraSil AP metal scavenger was added and stirred for 30 minutes. The suspension was filtered, evaporated and subjected to HPLC purification to give the compound in >99 % purity. ^{1}H NMR (400 MHz, D$_2$O) δ 8.08 (d, J = 6.2 Hz, 4H), 7.61 (d, J = 1.7 Hz, 2H), 7.02 – 6.98 (m, 5H). ^{13}C NMR (101 MHz,) δ 172.9, 148.6, 146.7, 137.6, 136.71, 127.7, 126.4, 121.1. HRMS (ESI) m/z: [M-H$^+$] calculated for C$_{17}$H$_{12}$O$_2$N$_2$ 275.0826; found 275.0826.

Author Contributions

Conceived and designed the experiment: HKSL BAL TC AB. Performed the experiments: BAL TC YG HKSL Analyzed the data: BAL TC HKSL YG AB. Wrote the paper: BAL HKSL TC. All authors have given approval to the final version of the manuscript.

Acknowledgements

Abbreviations

AMP, ampicillin; CHL, chloramphenicol; TEV, Tobacco Etch Virus; NHC, N-hydroxysuccinimide; EDC, 1-ethyl-3-(3-dimethylaminopropyl)carbodiimide; SPR, surface plasmon resonance; OXA, oxacillinase; RU, Response Units; PAINS, Pan-Assay Interference compounds.

PDB Accession codes

Coordinates and structure factors of tOXA-48:**1**, tOXA-48:**2**, tOXA-48:**3** and tOXA-48:**17** have been deposited in the Protein Data Bank with accession numbers 5DVA, 5DTS, 5DTT and 5DTK.

Corresponding author information

Hanna-Kirsti S. Leiros, E-mail: hanna-kirsti.leiros@uit.no, Phone: (+47) 77 64 57 06

Supporting information Available:

HPLC analysis of compound **17**, enzyme kinetic steady-state plots, SPR sensorgrams and steady-state plots for compounds **12** and **13**, and logarithmic binding affinities and inhibition constants with standard errors.

References

(1)   ECDC/EMEA Joint Working Group. *The bacterial challenge : time to react*. EMEA/576176/2009: Stockholm, Sweden 2009.

(2)   Papp-Wallace, K. M.; Endimiani, A.; Taracila, M. A.; Bonomo, R. A. Carbapenems: past, present, and future. *Antimicrob. Agents Chemother.* **2011**, *55*, 4943–4960.

(3)   Poirel, L.; Potron, A.; Nordmann, P. OXA-48-like carbapenemases: the phantom

menace. *J. Antimicrob. Chemother.* **2012**, *67*, 1597–1606.

(4)   Mathers, A. J.; Hazen, K. C.; Carroll, J.; Yeh, A. J.; Cox, H. L.; Bonomo, R. A.; Sifri,

C. D. First clinical cases of OXA-48-producing carbapenem-resistant *Klebsiella*

pneumoniae in the United States: the "menace" arrives in the new world. *J. Clin.*

Microbiol. **2013**, *51*, 680–683.

(5)   Drawz, S. M.; Bonomo, R. a. Three decades of β-lactamase inhibitors. *Clin.*

Microbiol. Rev. **2010**, *23*, 160–201.

(6)   Danel, F.; Paetzel, M.; Strynadka, N. C. J.; Page, M. G. P. Effect of Divalent Metal

Cations on the Dimerization of OXA-10 and -14 Class D β-Lactamases from

Pseudomonas aeruginosa. *Biochemistry* **2001**, *40*, 9412–9420.

(7)   Vercheval, L.; Bauvois, C.; di Paolo, A.; Borel, F.; Ferrer, J.-L.; Sauvage, E.;

Matagne, A.; Frère, J.-M.; Charlier, P.; Galleni, M.; Kerff, F. Three factors that

modulate the activity of class D β-lactamases and interfere with the post-translational

carboxylation of Lys70. *Biochem. J.* **2010**, *432*, 495–504.

(8)   Golemi, D.; Maveyraud, L.; Vakulenko, S.; Samama, J. P.; Mobashery, S. Critical

involvement of a carbamylated lysine in catalytic function of class D β-lactamases.

Proc. Natl. Acad. Sci. U. S. A. **2001**, *98*, 14280–14285.

(9)   Toussaint, K. A.; Gallagher, J. C. β -Lactam/β-lactamase inhibitor combinations:

from then to now. *Ann. Pharmacother.* **2015**, *49*, 86–98.

(10)   Ehmann, D. E.; Jahic, H.; Ross, P. L.; Gu, R.-F.; Hu, J.; Durand-Réville, T. F.; Lahiri,

S.; Thresher, J.; Livchak, S.; Gao, N.; Palmer, T.; Walkup, G. K.; Fisher, S. L.

Kinetics of avibactam inhibition against Class A, C, and D β-lactamases. *J. Biol. Chem.* **2013**, *288*, 27960–27971.

(11)   Garber, K. A β-lactamase inhibitor revival provides new hope for old antibiotics. *Nat. Rev. Drug Discovery* **2015**, *14*, 445–447.

(12)   Lahiri, S. D.; Mangani, S.; Jahić, H.; Benvenuti, M.; Durand-Reville, T. F.; De Luca, F.; Ehmann, D. E.; Rossolini, G. M.; Alm, R. A.; Docquier, J.-D.; Jahic, H.; Benvenuti, M.; Durand-Reville, T. F.; De Luca, F.; Ehmann, D. E.; Rossolini, G. M.; Alm, R. A.; Docquier, J.-D. Molecular basis of selective inhibition and slow reversibility of Avibactam against class D carbapenemases: a structure-guided study of OXA-24 and OXA-48. *ACS Chem. Biol.* **2014**, *10*, 591–600.

(13)   Drawz, S. M.; Papp-Wallace, K. M.; Bonomo, R. a. New β-lactamase inhibitors: a therapeutic renaissance in an MDR world. *Antimicrob. Agents Chemother.* **2014**, *58*, 1835–1846.

(14)   Humphries, R. M.; Yang, S.; Hemarajata, P.; Ward, K. W.; Hindler, J. A.; Miller, S. A.; Gregson, A. First report of ceftazidime-avibactam resistance in a KPC-3 expressing *Klebsiella pneumoniae*. *Antimicrob. Agents Chemother.* **2015**, *59*, 6605–6607.

(15)   Papp-Wallace, K. M.; Winkler, M. L.; Taracila, M. A.; Bonomo, R. A. Variants of β-lactamase KPC-2 that are resistant to inhibition by Avibactam. *Antimicrob. Agents Chemother.* **2015**, *59*, 3710–3717.

(16)   Winkler, M. L.; Papp-Wallace, K. M.; Taracila, M. A.; Bonomo, R. A. Avibactam and inhibitor-resistant SHV β-lactamases. *Antimicrob. Agents Chemother.* **2015**, *59*, 3700–3709.

(17)   Congreve, M.; Chessari, G.; Tisi, D.; Woodhead, A. J. Recent developments in

         fragment-based drug discovery. *J. Med. Chem.* **2008**, *51*, 3661–3680.

(18)   Roughley, S. D.; Hubbard, R. E. How well can fragments explore accessed chemical

         space? A case study from heat shock protein 90. *J. Med. Chem.* **2011**, *54*, 3989–4005.

(19)   Danielson, U. Fragment library screening and lead characterization using SPR

         biosensors. *Curr. Top. Med. Chem.* **2009**, *9*, 1725–1735.

(20)   Navratilova, I.; Hopkins, A. L. Emerging role of surface plasmon resonance in

         fragment-based drug discovery. *Future Med. Chem.* **2011**, *3*, 1809–1820.

(21)   Baell, J. B.; Holloway, G. A. New substructure filters for removal of pan assay

         interference compounds (PAINS) from screening libraries and for their exclusion in

         bioassays. *J. Med. Chem.* **2010**, *53*, 2719–2740.

(22)   Giannetti, A. M.; Koch, B. D.; Browner, M. F. Surface plasmon resonance based

         assay for the detection and characterization of promiscuous inhibitors. **2008**, *4*, 574–

         580.

(23)   Giannetti, A. M. FROM EXPERIMENTAL DESIGN TO VALIDATED HITS A

         COMPREHENSIVE WALK-THROUGH OF FRAGMENT LEAD

         IDENTIFICATION USING SURFACE PLASMON RESONANCE. 1st ed.; Elsevier

         Inc.: Cambridge, Massachusetts, 2011; Vol. 493.

(24)   Lund, B. A.; Leiros, H.-K. S.; Bjerga, G. E. A high-throughput, restriction-free

         cloning and screening strategy based on *ccd*B-gene replacement. *Microb. Cell Fact.*

         2014, *13*, 38.

(25)   Petersen, T. N.; Brunak, S.; von Heijne, G.; Nielsen, H. SignalP 4.0: discriminating signal peptides from transmembrane regions. *Nat. Methods* **2011**, *8*, 785–786.

(26)   Antunes, N. T.; Lamoureaux, T. L.; Toth, M.; Stewart, N. K.; Frase, H.; Vakulenko, S. B. Class D β-lactamases: are they all carbapenemases? *Antimicrob. Agents Chemother.* **2014**, *58*, 2119–2125.

(27)   Docquier, J.-D.; Calderone, V.; De Luca, F.; Benvenuti, M.; Giuliani, F.; Bellucci, L.; Tafi, A.; Nordmann, P.; Botta, M.; Rossolini, G. M.; Mangani, S. Crystal structure of the OXA-48 β-lactamase reveals mechanistic diversity among class D carbapenemases. *Chem. Biol.* **2009**, *16*, 540–547.

(28)   O'Callaghan, C. H.; Morris, A.; Kirby, S. M.; Shingler, A. H. Novel method for detection of β-lactamases by using a chromogenic cephalosporin substrate. *Antimicrob. Agents Chemother.* **1972**, *1*, 283–288.

(29)   Bebrone, C.; Moali, C.; Mahy, F.; Rival, S.; Docquier, J. D.; Rossolini, G. M.; Fastrez, J.; Pratt, R. F.; Frère, J. M.; Galleni, M. CENTA as a chromogenic substrate for studying β-lactamases. *Antimicrob. Agents Chemother.* **2001**, *45*, 1868–1871.

(30)   Biacore^{TM} Assay Handbook; GE Healthcare Bio-Sciences AB: Uppsala, Sweden, 2012; p 40.

(31)   Congreve, M.; Carr, R.; Murray, C.; Jhoti, H. A "Rule of Three" for fragment-based lead discovery? *Drug Discovery Today* **2003**, *8*, 876–877.

(32)   Hopkins, A. L.; Groom, C. R.; Alex, A. Ligand efficiency: a useful metric for lead selection. *Drug Discovery Today* **2004**, *9*, 430–431.

(33) Hopkins, A. L.; Keserü, G. M.; Leeson, P. D.; Rees, D. C.; Reynolds, C. H. The role of ligand efficiency metrics in drug discovery. *Nat. Rev. Drug Discovery* **2014**, *13*, 105–121.

(34) Krissinel, E.; Henrick, K. Secondary-structure matching (SSM), a new tool for fast protein structure alignment in three dimensions. *Acta Crystallogr. Sect. D Biol. Crystallogr.* **2004**, *60*, 2256–2268.

(35) Beck, J.; Vercheval, L.; Bebrone, C.; Herteg-Fernea, A.; Lassaux, P.; Marchand-Brynaert, J. Discovery of novel lipophilic inhibitors of OXA-10 enzyme (class D β-lactamase) by screening amino analogs and homologs of citrate and isocitrate. *Bioorg. Med. Chem. Lett.* **2009**, *19*, 3593–3597.

(36) Docquier, J.-D.; Benvenuti, M.; Calderone, V.; Giuliani, F.; Kapetis, D.; De Luca, F.; Rossolini, G. M.; Mangani, S. Crystal structure of the narrow-spectrum OXA-46 class D β-lactamase: relationship between active-site lysine carbamylation and inhibition by polycarboxylates. *Antimicrob. Agents Chemother.* **2010**, *54*, 2167–2174.

(37) King, D. T.; King, A. M.; Lal, S. M.; Wright, G. D.; Strynadka, N. C. J. Molecular mechanism of Avibactam-mediated β-lactamase inhibition. *ACS Infect. Dis.* **2015**, *1*, 175–184.

(38) Szarecka, A.; Lesnock, K. R.; Ramirez-Mondragon, C. A.; Nicholas, H. B.; Wymore, T. The class D β-lactamase family: residues governing the maintenance and diversity of function. *Protein Eng. Des. Sel.* **2011**, *24*, 801–809.

(39) Christopeit, T.; Carlsen, T. J. O.; Helland, R.; Leiros, H.-K. S. Discovery of novel inhibitor scaffolds against the metallo-β-lactamase VIM-2 by surface plasmon resonance (SPR) based fragment screening. *J. Med. Chem.* **2015**, *58*, 8671–8682.

(40) Ulrich, A.; Andersen, K. R.; Schwartz, T. U. Exponential megapriming PCR (EMP) cloning-seamless DNA insertion into any target plasmid without sequence constraints. *PLoS One* **2012**, *7*, e53360.

(41) Unger, T.; Jacobovitch, Y.; Dantes, A.; Bernheim, R.; Peleg, Y. Applications of the Restriction Free (RF) cloning procedure for molecular manipulations and protein expression. *J. Struct. Biol.* **2010**, *172*, 34–44.

(42) Studier, F. W. Protein production by auto-induction in high-density shaking cultures. *Protein Expression Purif.* **2005**, *41*, 207–234.

(43) Kabsch, W. XDS. *Acta Crystallogr. D. Biol. Crystallogr.* **2010**, *66*, 125–132.

(44) Evans, P. R.; Murshudov, G. N. How good are my data and what is the resolution? *Acta Crystallogr. D. Biol. Crystallogr.* **2013**, *69*, 1204–1214.

(45) McCoy, A. J.; Grosse-Kunstleve, R. W.; Adams, P. D.; Winn, M. D.; Storoni, L. C.; Read, R. J. Phaser crystallographic software. *J. Appl. Crystallogr.* **2007**, *40*, 658–674.

(46) Afonine, P. V; Grosse-Kunstleve, R. W.; Echols, N.; Headd, J. J.; Moriarty, N. W.; Mustyakimov, M.; Terwilliger, T. C.; Urzhumtsev, A.; Zwart, P. H.; Adams, P. D. Towards automated crystallographic structure refinement with phenix.refine. *Acta Crystallogr. D. Biol. Crystallogr.* **2012**, *68*, 352–367.

(47) Smart, O. S.; Womack, T. O.; Sharff, A.; Flensburg, C.; Keller, P.; Paciorek, W.; Vonrhein, C.; Bricogne, G. Grade, version 1.102. Global Phasing 2014.

(48) Emsley, P.; Lohkamp, B.; Scott, W. G.; Cowtan, K. Features and development of *Coot*. *Acta Crystallogr. Sect. D Biol. Crystallogr.* **2010**, *66*, 486–501.

(49)   Liebschner, D. *Phenix.polder* - A tool for calculating difference maps around atom

        selections by excluding the bulk solvent mask. The Phenix Project: Berkeley,

        California 2016.

(50)   Schrödinger LLC. The *PyMOL* Molecular Graphics System. New York, NY August

        2014.

(51)   Laskowski, R. A.; Swindells, M. B. LigPlot+: multiple ligand–protein interaction

        diagrams for drug discovery. *J. Chem. Inf. Model.* **2011**, *51*, 2778–2786.

(52)   Sherman, W.; Day, T.; Jacobson, M. P.; Friesner, R. A.; Farid, R. Novel procedure

        for modeling ligand/receptor induced fit effects. *J. Med. Chem.* **2006**, *49*, 534–553.

(53)   Tominaga, M.; Suzuki, K.; Kawano, M.; Kusukawa, T.; Ozeki, T.; Sakamoto, S.;

        Yamaguchi, K.; Fujita, M. Finite, spherical coordination networks that self-organize

        from 36 small components. *Angew. Chem. Int. Ed. Engl.* **2004**, *43*, 5621–5625.

Tables and Figures

Table 1 Steady- state enzyme kinetic parameters of nOXA-48 with penicillins, cephalosporin, carbapenems and reporter substrates, with standard errors. Kinetic parameters for tOXA-48 with the reporter substrate nitrocefin is also included as comparison.

Table 2 Molecular structure, binding affinity (K_D) and IC_{50} values for the fragments identified during the screening campaign. The LE is also calculated from the K_D value using the formula $LE = (RTpK_D) \div N_{heavy\ atom}$. n.f.: **N**ot **F**ound. Standard errors are given in Table S1.

Table 3 Binding affinities (K_D), IC_{50} values for compound **11-17**. Standard errors are given in Table S1.
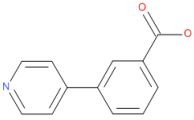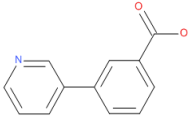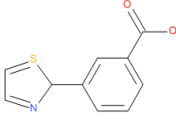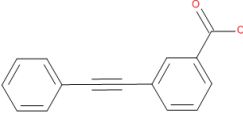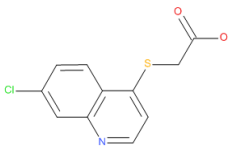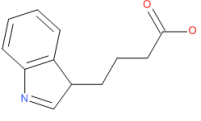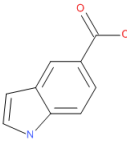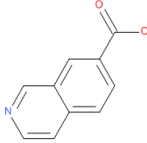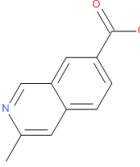
Table 4 Data collection and refinement statistics for the complex-structures of tOXA-48 in complex with compounds **1**, **2**, **3** and **17**. Statistics for the highest-resolution shell are shown in parentheses

Table 5 Primers used in the cloning of the new tOXA-48 gene construct. The vector-specific sequence is in bold, the TEV protease cleavage site sequence is in italic and OXA-48 gene-specific sequence is underlined.

Table 1

Substrate	Enzyme	K_m (µM)	k_{cat} (s^{-1})	k_{cat}/K_m (M^{-1}s^{-1})
Penicillin				
Ampicillin	nOXA-48	150±30	560±30	3.7×10^6
Benzylpenicillin	nOXA-48	700±300	8000±1100	1.1×10^7
Cephalosporin				
Cefepime	nOXA-48	300±110	9±2	3.0×10^4
Carbapenem				
Imipenem	nOXA-48	7.9±0.1	4.5±0.8	5.7×10^5
Meropenem	nOXA-48	1.0±0.2	0.098±0.005	9.8×10^4
Reporter substrates				
Nitrocefin	tOXA-48	150±13	2300±100	1.5×10^7
Nitrocefin	nOXA-48	90±11	1500±80	1.7×10^7
CENTA	nOXA-48	24±2	0.66±0.01	2.8×10^4

Table 2

No.	Compound	K_D (μM)	IC_{50} (μM)	LE (kcal per mole per heavy atom)
1		280	250	0.33
2		280	240	0.33
3		310	250	0.35
4		n.f.	480	n.f
5		n.f.	220	n.f.
6		430	480	0.31
7		1380	1390	0.33
8		1180	2200	0.32
9		700	1020	0.32
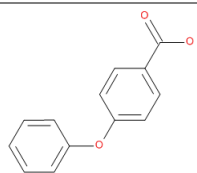
| 10 | | 660 | 870 | 0.28 |

Table 3
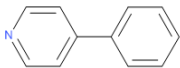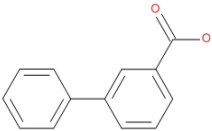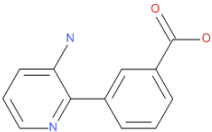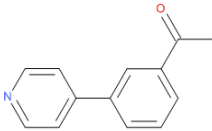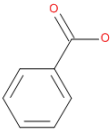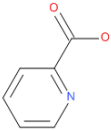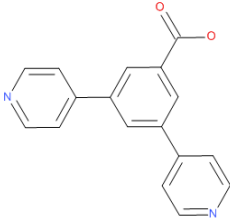
No.	Compound	K_D (μM)	IC_{50} (μM)
11		> 1 000	>2 000
12		370	260
13		330	180
14		> 1 000	>2 000
15		> 1 000	>2 000
16		> 1 000	>2 000
17		50	18

Table 4

	OXA-48:1	OXA-48:2	OXA-48:3	OXA-48:17
PDB entry	5DVA	5DTS	5DTT	5DTK
Data Collection	Bessy BL14.1	Bessy BL14.1	Bessy BL14.1	Bessy BL14.1
Wavelength (Å)	0.9184	0.9184	0.9184	0.9184
Resolution range (Å)	19.95 - 2.50	54.30 - 1.94	45.96 - 2.10	43.86 - 1.60
	(2.59 - 2.50)	(2.01 - 1.94)	(2.18 - 2.10)	(1.66 - 1.60)
Space group	P 21 21 21	P 21 21 21	P 21 21 21	P 21
Unit-cell	91.04	89.60	88.37	45.52
(a,b,c (Å))	109.66	109.63	107.62	124.31
γ (°)	124.24	125.01	124.55	108.74
				98.26
Unique reflections	43599 (4315)	89748 (7698)	69611 (6874)	156931 (15661)
Multiplicity	2.0 (2.0)	6.0 (5.0)	3.7 (3.8)	3.4 (3.5)
Completeness (%)	99.0 (100.0)	98.0 (85.16)	99.0 (100.0)	100.0 (100.0)
Mean I/sigma(I)	4.00 (1.80)	4.67 (1.29)	6.35 (1.54)	11.78 (1.70)
Wilson B-factor (Å^2)	28.48	22.90	22.25	16.05
R_{meas}	0.1164 (0.4236)	0.2112 (0.9338)	0.1881 (0.9246)	0.086 (0.9140)
$CC_{1/2}$	0.994 (0.919)	0.986 (0.705)	0.993 (0.644)	0.998 (0.638)
Refinement				
R_{work}	0.2245 (0.2948)	0.2388 (0.3647)	0.2014 (0.3120)	0.1460 (0.2667)
R_{free}	0.2831 (0.3248)	0.2745 (0.3850)	0.2463 (0.3329)	0.1744 (0.3035)
RMS bonds (Å)	0.002	0.002	0.002	0.008
RMS angles(°)	0.50	0.49	0.50	0.95
Clashscore	2.98	3.14	1.91	2.28

<B-factors> (Å^2)	39.68	32.60	28.69	24.61
Protein	39.79	31.84	27.56	22.28
Ligands	37.36	34.78	27.52	39.53
Solvent	38.54	38.99	35.46	38.51
Occupancies Ligands	0.4-0.9	0.7	0.7-0.9	0.7-0.8

Table 5

Primer name	Sequence (5'-3')
OXA-48 fwd	**GTTTGTA**C*GGTGAGAATCTTTATTTTCAGGG*<u>TAAGGAATGGCAAGAAAACAAAAGT</u>
OXA-48 rev	**GGCTTTGTTAGCAGCCTCGAATCA**<u>CTAGGGAATAATTTTTTCCTGTTTGAG</u>
TEV protease cleavage site fwd	**ACCATCACCTCGAATCAACAAGTTTGTA**C*GGTGAGAATCTTTATTTTCAGGGT*t
TEV protease cleavage site rev	**GGCTTTGTTAGCAGCCTCGAATCA***ACCCTGAAAATAAAGATTCTCACC*G
EMP R2-primer	**TTGTTGATTCGAGGTGATGGTGAT**

Figure legends

Figure 1 A) Sensorgrams for the interaction between meropenem and tOXA-48 in the presence (green) and absence (yellow) of 50 mM bicarbonate. B) SPR-sensorgrams (solid lines) for the interaction of meropenem with tOXA-48 including bicarbonate. Meropenem was injected in a 2-fold concentration series (62.5 nM-32 μM), the data were fitted to a one binding site model (shown as symbols) yielding $k_a = 4 \times 10^4$ $M^{-1}s^{-1}$, $k_d = 0.3463$ s^{-1} and the binding affinity (K_D) was determined to be 0.85 μM.

Figure 2 SPR sensorgrams and steady-state plots for the binding of fragments **1-10** to tOXA-48. 2-fold dilution series from (118-900 μM) were used to determine the K_D. Steady state values were plotted against the concentration. The data, except for compound **4** and **5**, were fitted to 1:1 interaction model and the K_D was calculated.

Figure 3 IC_{50}-plots of fragments **1-10** inhibiting nitrocefin breakdown by nOXA-48, based on non-linear-regression analysis. The determined IC_{50} values are indicated for each fragment

Figure 4 Crystal structures of tOXA-48 (green) in complex with fragments (magenta). Two conformations are shown for compound **1** in panel A-C and only one protein chain for compound **2** (panel D-E) and **3** (panel F-G). The F_o-F_c maps are contoured at at +2.5σ. and the refined structures are depicted (left panles) together with a schemactic diagram of the protein-ligand interactions generated in Ligplot+ (right panles).

Figure 5 A) SPR sensorgrams and B) steady-state plot for the binding of compound **17** to tOXA-48. A 2-fold dilution series (1.8 μM-900 μM) were used to determine the K_D of 50 μM. C) IC_{50}-plot of compound **17** inhibiting nitrocefin breakdown by nOXA-48, based on non-linear-regression analysis. The determined IC_{50} value for compound **17** is 18 μM. D) Crystal structure of compound **17** (magenta) in complex with tOXA-48 (green). The F_o-F_c

map is contoured at +2.5σ. E) Schemactic diagram of the protein-ligand interactions from

tOXA-48 to compound **17** generated by Ligplot+ with standard settings.
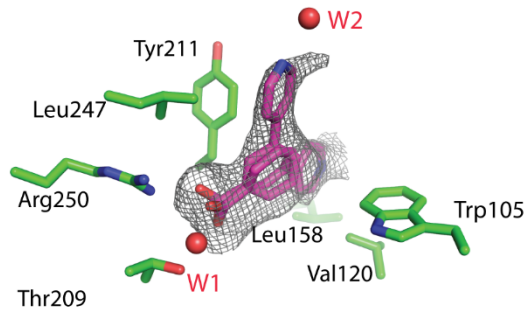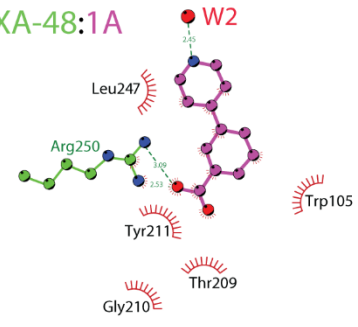
Figure legends
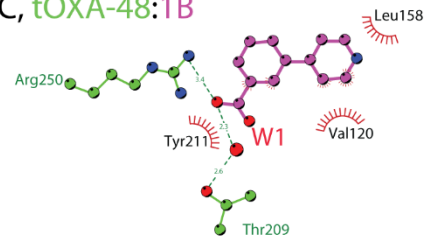
Figure 1
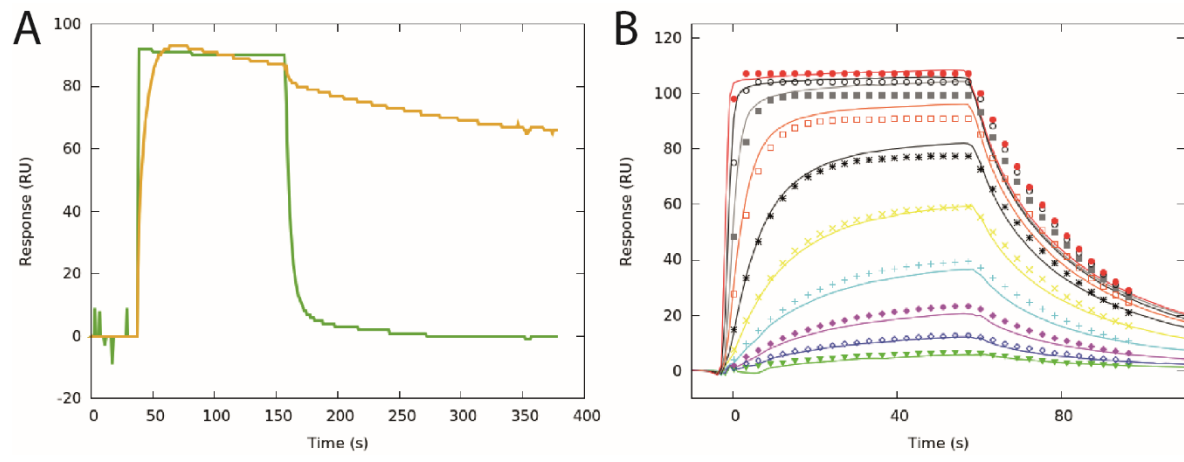
Figure 2
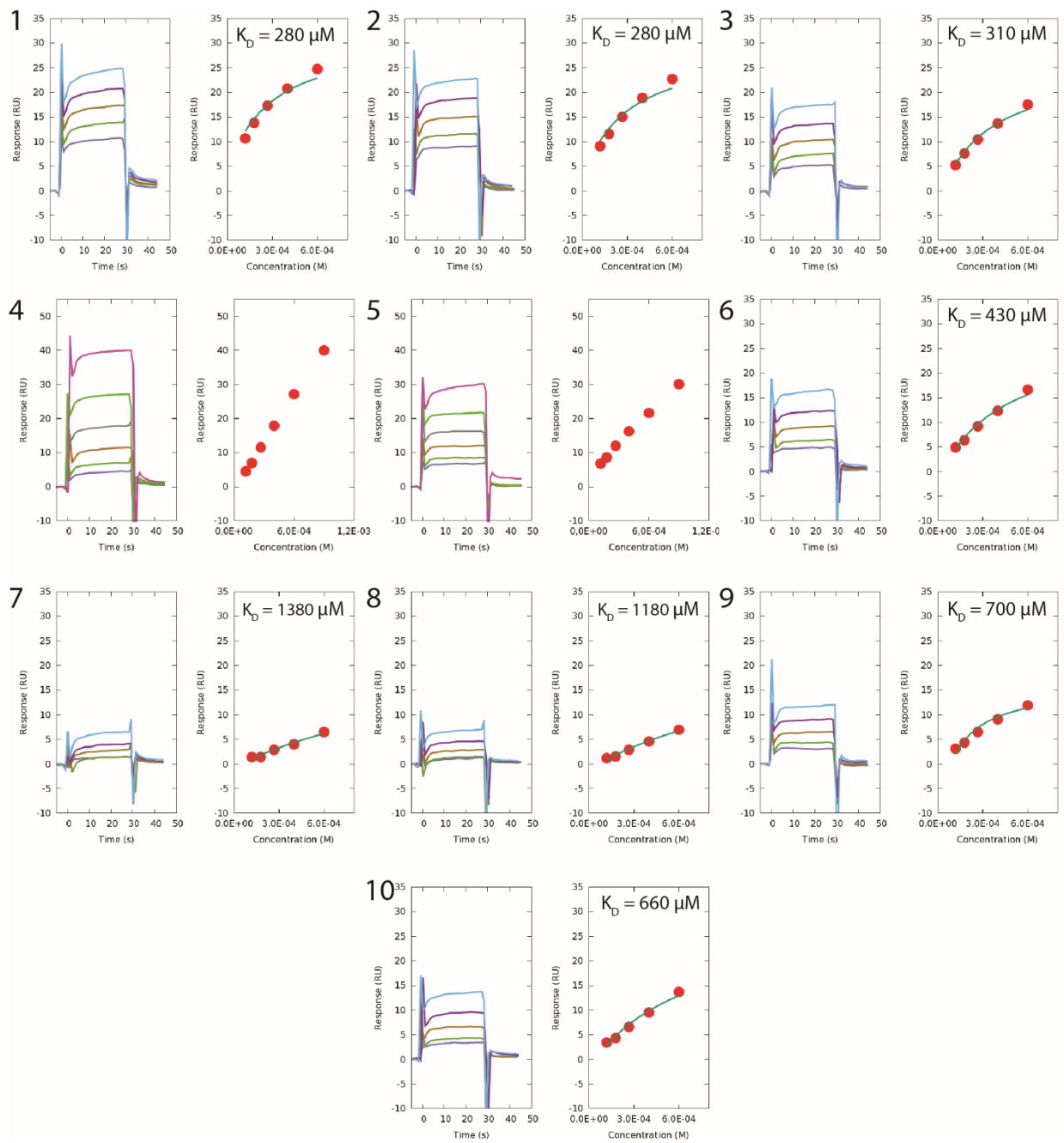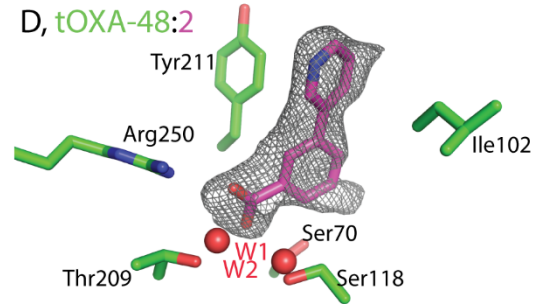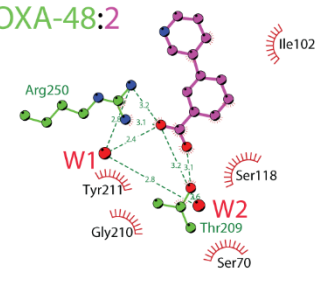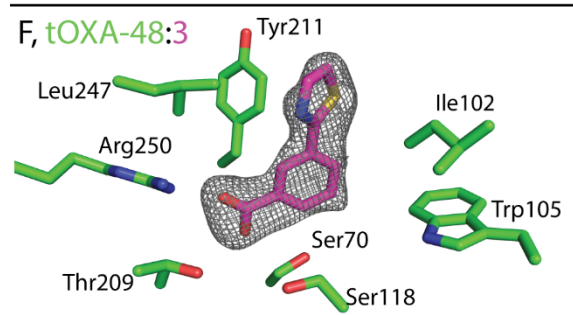
Figure 3
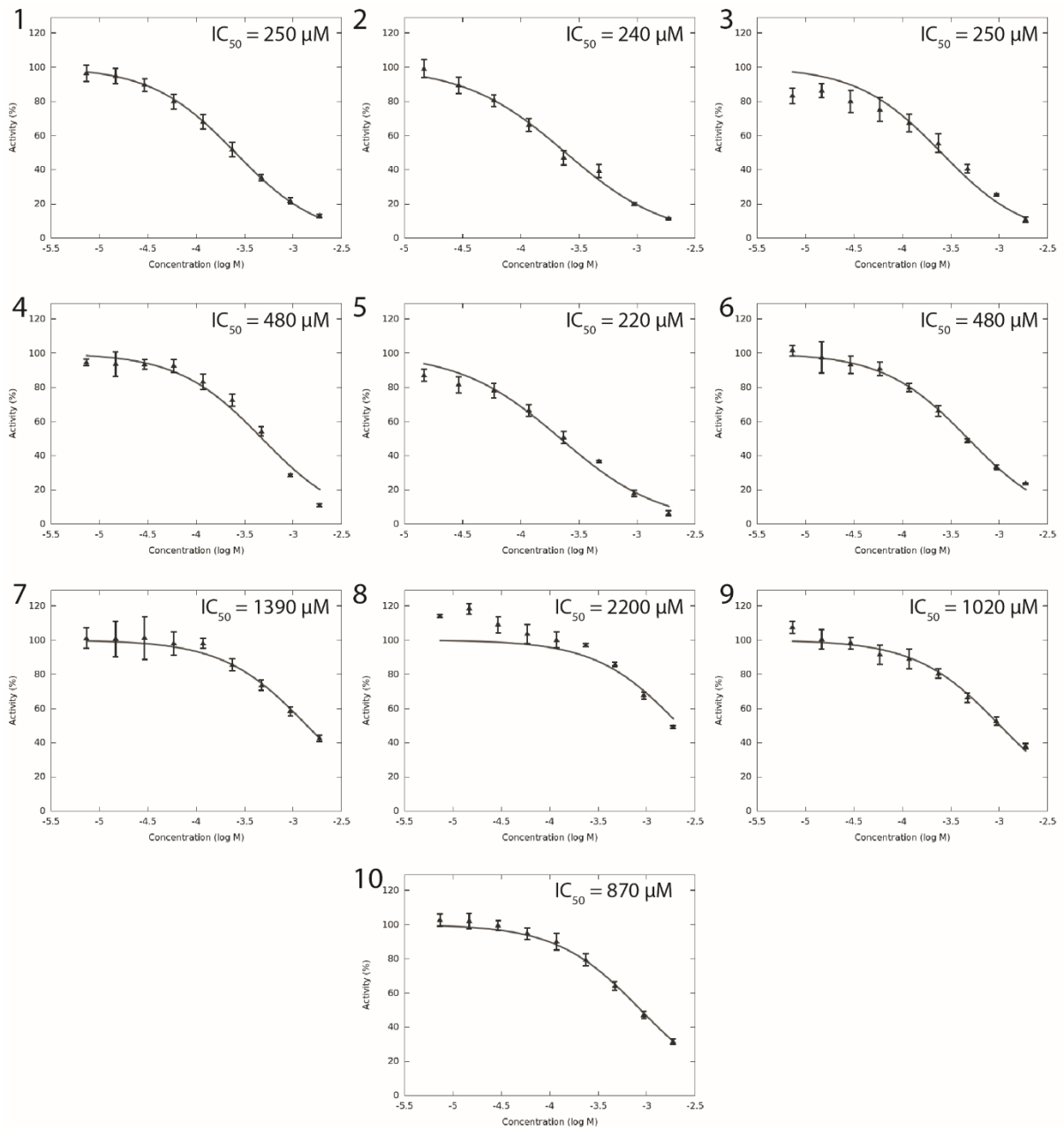
Figure 4

A, tOXA-48:1

B, tOXA-48:1A

C, tOXA-48:1B

D, tOXA-48:2

E, tOXA-48:2

F, tOXA-48:3

G, tOXA-48:2
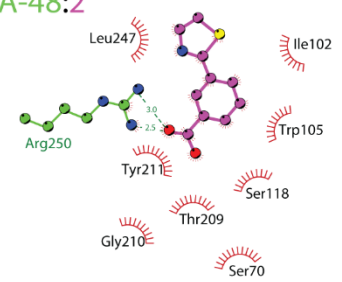
Figure 5

Scheme 1 Reaction scheme for the synthesis of compound **17.**
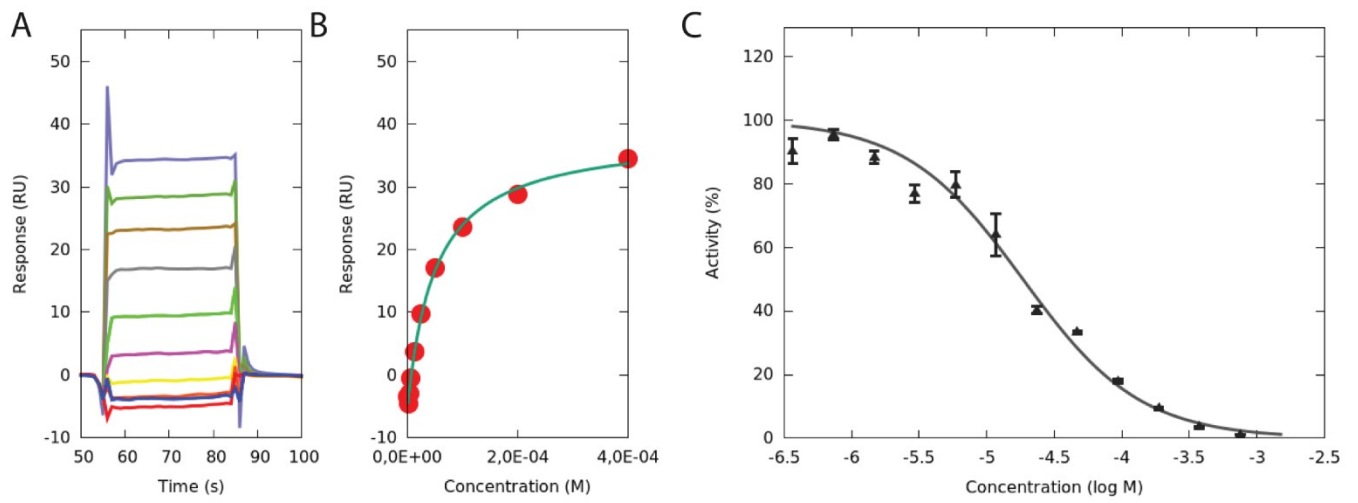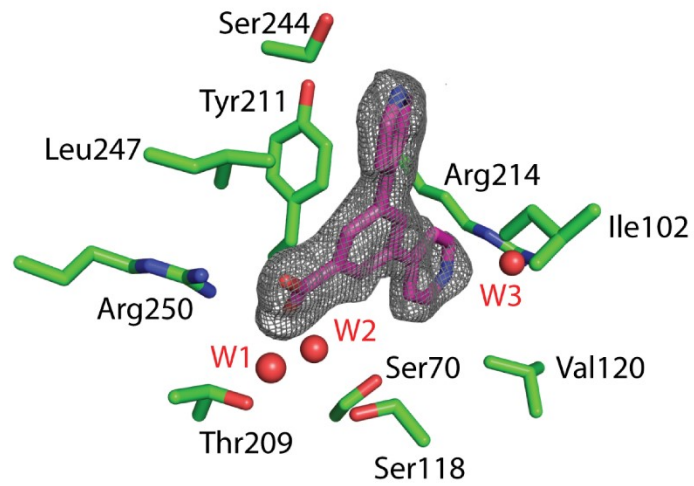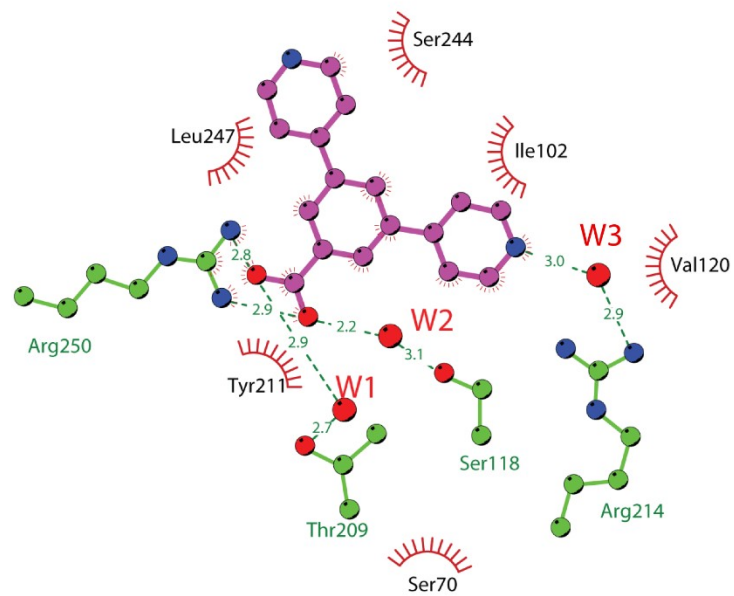
Scheme 1
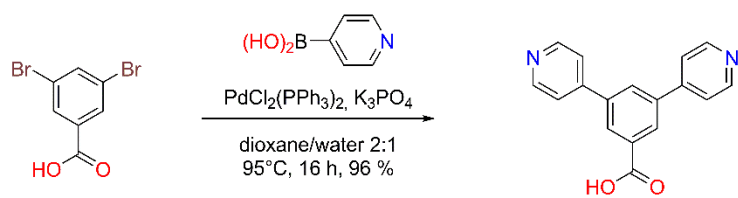
TOC graphic
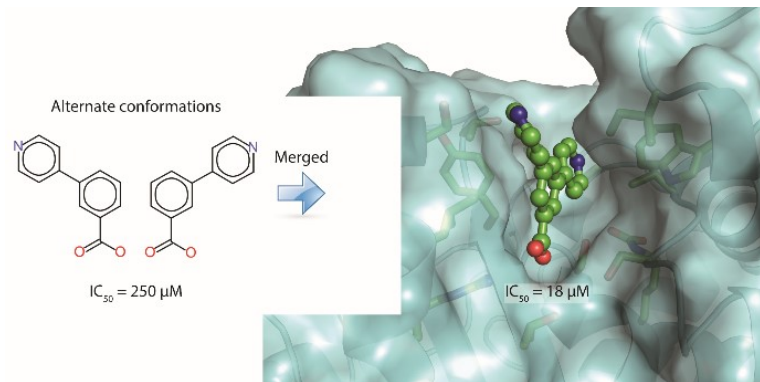
Alternate conformations

Merged

$IC_{50} = 250 \ \mu M$

$IC_{50} = 18 \ \mu M$

Screening and design of inhibitor scaffolds for the antibiotic resistance oxacillinase-48 (OXA-48) through surface plasmon resonance screening.

Bjarte Aarmo Lund[1], Tony Christopeit[1], Yngve Guttormsen[2], Annette Bayer[2] and Hanna-Kirsti S. Leiros[1,]*

[1]The Norwegian Structural Biology Centre (NorStruct), Department of Chemistry, UiT The Arctic University of Norway, Tromsø, Norway

[2]Department of Chemistry, UiT The Arctic University of Norway, Tromsø, Norway

* Corresponding author:

Hanna-Kirsti S. Leiros, E-mail: hanna-kirsti.leiros@uit.no, Phone: (+47) 77 64 57 06
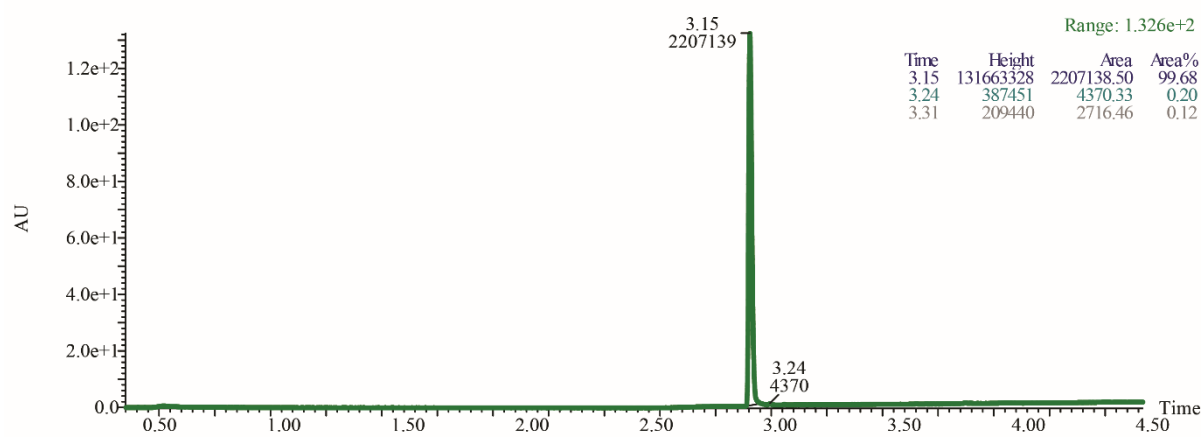
Table of Contents

Figure S1 HPLC analysis of compound **17** after synthesis confirms the purity of the compound to be 99.7%.
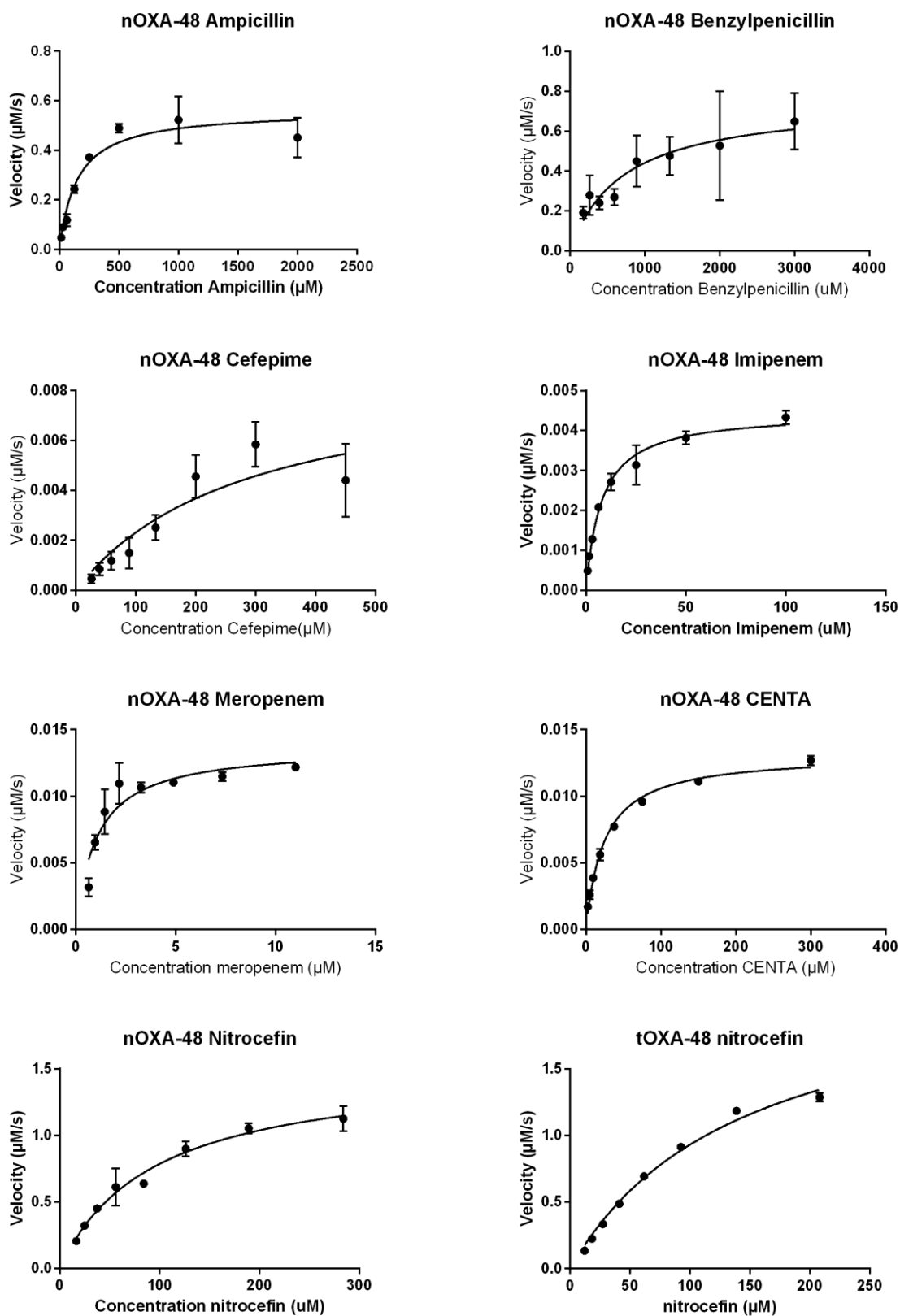
Figure S2 Enzyme kinetic steady-state plots for nOXA-48 with penicillins, one cephalosporin, carbapenems and reporter substrates. Steady state plot of tOXA-48 with the reporter substrate nitrocefin is also shown.
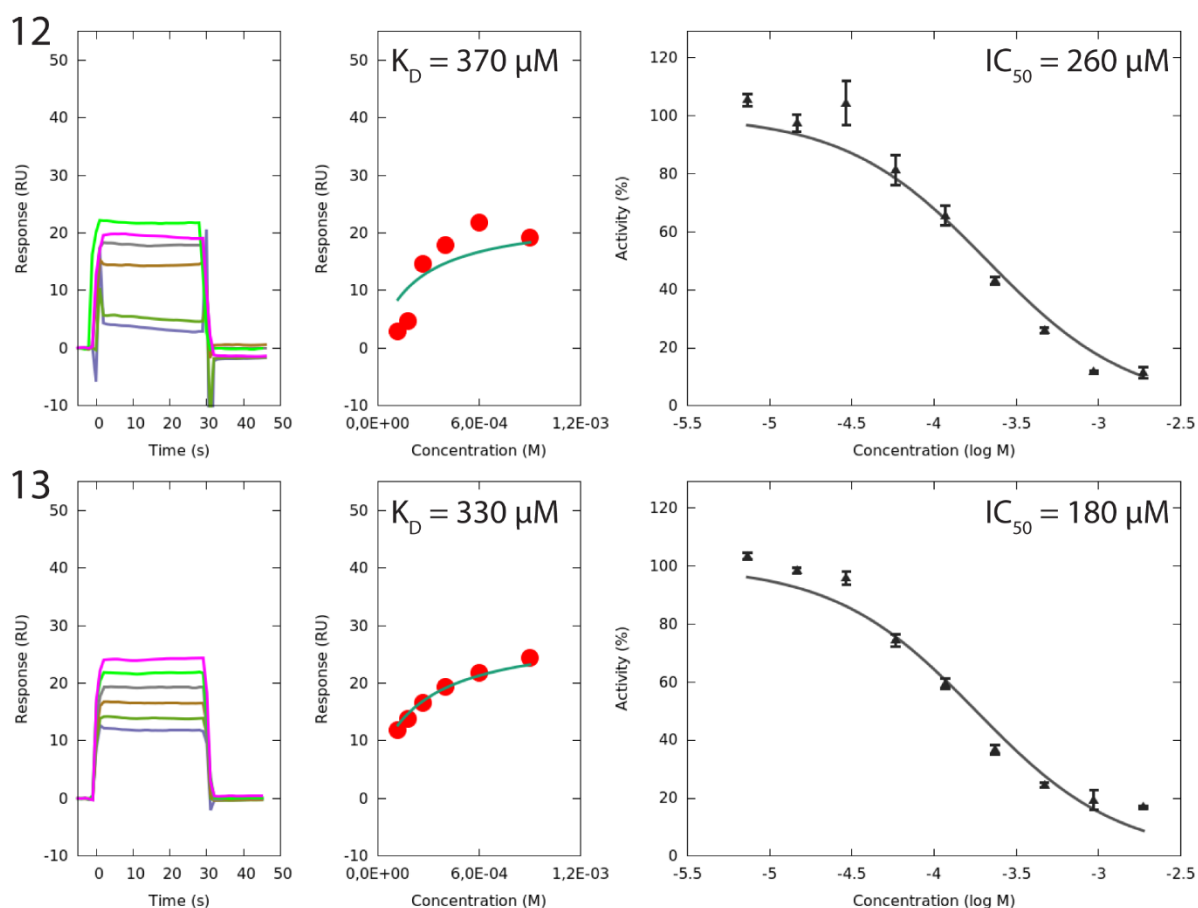
Figure S3 Sensorgrams (left panels) and steady-state plots (middle panels) for the binding of compounds **12** and **13** binding to tOXA-48. 2-fold dilution series from (118-900 µM) were used to determine the K_D. Steady state values were plotted against the concentration. The data were fitted to 1:1 interaction model and the K_D was calculated. IC_{50}-plots (right panels) of compounds **12** and **13** inhibiting nitrocefin breakdown by nOXA-48, based on non-linear-regression analysis. The determined IC_{50} values are indicated for both compounds.

Table S1 Logarithmic transformed binding affinities (K_D) and inhibition constants (IC_{50}) for the compounds **1-10** and **12,13** and **17**. Units are Log molar. The standard errors are given are calculated from least two independent measurements.

Compound no.	pK_D	pIC_{50}
1	3.6 ± 0.2	3.60 ± 0.03
2	3.6 ± 0.2	3.62 ± 0.04
3	3.5 ± 0.1	3.60 ± 0.06
4		3.32 ±0.04
5		3.66 ± 0.04
6	3.4 ± 0.2	3.32 ± 0.04
7	2.9 ± 0.1	2.86 ± 0.07
8	2.9 ± 0.1	2.66 ± 0.08
9	3.16 ± 0.02	2.99 ± 0.04
10	3.2 ± 0.1	3.06 ± 0.03
12	3.4 ± 0.1	3.68 ± 0.05
13	3.5 ± 0.2	3.75 ± 0.04
17	4.30 ± 0.03	4.73 ± 0.03